DEUTSCHES ELEKTRONEN-SYNCHROTRON DESY

DESY 86-067
June 1986

RECENT RESULTS FROM ARGUS ON PRODUCTION AND DECAY OF HEAVY PARTICLES

by

D. B. MacFarlane

Department of Physics, University of Toronto, Toronto, Ontario, Canada

H. Schröder

Deutsches Elektronen-Synchrotron DESY, Hamburg, Germany

ISSN 0418-9833

NOTKESTRASSE 85 · 2 HAMBURG 52

To be sure that your preprints are promptly included in the
HIGH ENERGY PHYSICS INDEX ,
send them to the following address (if possible by air mail) :

DESY
Bibliothek
Notkestrasse 85
2 Hamburg 52
Germany

DESY 86-067 ISSN 0418-9833
June 1986

RECENT RESULTS FROM ARGUS ON PRODUCTION AND DECAY OF HEAVY PARTICLES.[†]

David B. MacFarlane
Department of Physics,
University of Toronto,
Toronto, Ontario, Canada

and

Henning Schröder
DESY, Hamburg, Germany

(representing the ARGUS collaboration*)

ABSTRACT. Recent results are reported from data accumulated by the ARGUS experiment, operating at around 10 GeV centre-of-mass energies in the DORIS II e^+e^- storage ring at DESY. Signals for both the octet states Λ, Σ^0 and Ξ^- and the decuplet states $\Sigma^{*\pm}$, $\Xi^{*0}(1530)$ and Ω^- have been observed. Baryon rates from direct $\Upsilon(1S)$ decays are found to be enhanced by a factor of 3 over the continuum. The decay $D^0 \to \overline{K}^0\phi$ has been investigated with higher statistics yielding a branching ratio of $Br(D^0 \to \overline{K}^0\phi) = (1.18 \pm 0.25 \pm 0.17)\%$. B-mesons have been reconstructed in decay modes involving D^{*+}, J/Ψ and Ψ' mesons. The decay $\tau \to \omega\pi\nu$ has been observed for the first time with a preliminary branching ratio of $Br(\tau \to \omega\pi\nu) = (1.7 \pm 0.4)\%$.

[†]Talks presented at the XXIst Rencontre de Moriond, Les Arcs, France.

1. Introduction

Results from the ARGUS collaboration are reported, based on study of a large sample of e^+e^- annihilation events accumulated at the e^+e^- storage ring DORIS II. The data comprise an integrated luminosity of 152 pb^{-1}, collected on the $\Upsilon(1S)$, $\Upsilon(2S)$ and $\Upsilon(4S)$ and in the nearby continuum. Relative production rates for both spin 1/2 and spin 3/2 hyperons are presented, including observation of the Ω^-. The high rate for continuum charm production has been exploited in a detailed investigation of the decay channel $D^0 \to \overline{K}^0\phi$, which is expected [1] to proceed at a substantial rate only via flavour annihilation through W exchange (Figure 1). Observation of this channel is of critical importance for our understanding of the competing mechanisms for hadronic weak decays of charm mesons. The subsample of 59 pb^{-1} taken on the $\Upsilon(4S)$ has been used for a study of exclusive and inclusive B decays leading to final states containing charm, such as $B \to D^* + n\pi$ and $B \to J/\Psi X$. Finally, in a continuation of our investigations of tau lepton properties, we report the first observation of the decay $\tau \to \omega\pi\nu$.

ARGUS is a 4π solenoidal spectrometer, with good charged and neutral particle detection. Particle identification is made possible both by measurement of mean dE/dx loss in the central drift chamber, and by a system of time-of-flight counters. From this information, a likelihood ratio is constructed which describes the relative probability for each of the possible particle assignments. If the reconstruction procedure requires a specific particle type, then all tracks for which this probability exceeds 5% are considered acceptable candidates. The electromagnetic calorimeter, located inside the magnet coils, allows photon reconstruction down to energies below 50 MeV. A more detailed description of the experiment can be found in reference 2.

2. Baryon production

The long lifetime of the Λ and K^0_S permits the use of vertex information as a means of reducing backgrounds. The procedure used for finding vertices is a necessarily iterative process, performed by making an unconstrained fit of a common point of origin to a given set of measured tracks and rejecting those tracks which contribute large χ^2. A fit is considered successful if the distances of closest approach to the common origin are less than seven standard deviations for all tracks. The algorithm is first applied in the construction of a primary vertex, using all tracks, then to secondary vertices, using tracks which have been rejected from the primary vertex. A final step is to attempt the reconstruction of secondary

vertices from combinations of remaining unassigned tracks with tracks already included in a vertex.

Figure 2 shows the invariant mass distribution for $p\pi^-$ combinations [3] from reconstructed secondary vertices. The prominent Λ peak contains 27330 ± 195 entries, as determined by a fit using the sum of two gaussians to account for the dependence of the resolution on momentum and decay point. The division of the number of observed Λ's among data taken on the various Υ resonances and in the nearby continuum can be found in Table 1. Subtracting the continuum and vacuum polarization contributions to the signal on the $\Upsilon(1S)$, we find that the rate of Λ production per event from $\Upsilon(1S)$ decays is 2.9 ± 0.4 times that for the continuum. The enhancement of the baryon rate on the $\Upsilon(1S)$ was first observed by DASP II [4], and is in agreement with results reported by CLEO [5].

For purposes of reconstructing higher mass hyperons, all Λ candidates within 3 sigma of the nominal Λ mass, and with momenta above 200 MeV/c, were subject to a mass constraint fit and used to form mass combinations. Shown with the open histogram in figure 3a is the mass distribution of $\Lambda\pi^-$ combinations with momenta greater than 400 MeV/c, but with no vertex requirement for the π^-, because of the relatively long average flight distance of the Ξ^-. A signal of 1885 ± 86 events is observed at the Ξ^- mass, divided among the resonance and continuum data subsets as shown in Table 1. Once again, the production rate for baryons per event from direct $\Upsilon(1S)$ decays is found to be enhanced over the continuum, for the Ξ^- by a factor of 2.9 ± 0.9.

Energy	Luminosity [pb^{-1}]	N[Λ]	N[Ξ^-]	N[Ξ^{*0}]
$\Upsilon(1S)$	21.7	11430 ± 120	766 ± 52	121 ± 27
$\Upsilon(2S)$	36.2	8810 ± 110	650 ± 54	90 ± 26
$\Upsilon(4S)$	59.0	5070 ± 90	333 ± 32	56 ± 17
Continuum	26.9	2020 ± 60	136 ± 28	8 ± 9
Total	143.8	27330 ± 200	1885 ± 86	279 ± 46

Table 1. Observed number of baryons on- and off-resonance.

In order to study $\Sigma^{*\pm}$ production, $\Lambda\pi^\pm$ combinations were used with the requirement that the $\pi^\pm$ fit to the primary event vertex, but with no momentum cut. Figure 3a (hatched histogram) and b show the resulting mass distributions. The Ξ^- signal is still visible, along with a broad enhancement in both figures corresponding to the Σ^{*-} and Σ^{*+} respectively. The solid lines are the result of a fit with a polynomial background, a gaussian for the Ξ^- and a relativistic Breit-Wigner of width 40(35) MeV/c^2 for the $\Sigma^{*-}(\Sigma^{*+})$. The number of Σ^{*-} and Σ^{*+} events was obtained by integrating the fitted Breit-Wigner between 1.35 and 1.42 GeV/c^2, yielding 721 ± 93 and 793 ± 101 entries respectively. Correcting for efficiency and the missing tails of the Breit-Wigner, the following ratios for decuplet-to-octet baryon production are obtained:

$$\Sigma^{*-}/\Lambda = 0.047 \pm 0.006^{+0.006}_{-0.005}$$

$$\Sigma^{*+}/\Lambda = 0.052 \pm 0.007^{+0.006}_{-0.004}$$

The sum of the two ratios is well within the limit reported by TASSO [6], but is considerably smaller than the value of $0.32 \pm 0.14 \pm 0.08$ obtained by TPC [7].

A search for the $\Xi^{*0}(1530)$, also a decuplet state, has been made in the $\Xi^-\pi^+$ mass spectrum (Figure 4). For this purpose, a Ξ^- was defined as a $\Lambda\pi^-$ combination lying within ± 20 MeV/c^2 of the nominal Ξ^- mass, and with momentum greater than 400 MeV/c. These candidates were then subject to a mass constraint fit, before being combined with the π^+. The prominant $\Xi^{*0}(1530)$ peak corresponds to 279 ± 46 events. Table 1 once more shows the division of the signal among the subsets of the data on- and off-resonance. In order to compute the $\Upsilon(1S)$ direct rate, the combined $\Upsilon(4S)$ and continuum signals were used for the continuum subtraction. By this means, the inclusive rate for $\Xi^{*-}(1530)$ production from $\Upsilon(1S)$ decays was found to be a factor of 3.3 ± 1.1 times the continuum rate. Averaging over all data, the ratio of $\Xi^{*0}(1530)$ to Ξ^- production is $0.26 \pm 0.04^{+0.04}_{-0.02}$. This is well in excess of the limit of 16% at the 90% CL reported by CLEO [8].

Evidence for Ω^- production can be seen in the ΛK^- mass distribution shown in Figure 5. The observed signal of 53 ± 16 events at the Ω^- mass corresponds to a Ω^-/Λ ratio of $(5.4 \pm 1.8 \pm 1.2) \times 10^{-3}$. Using the present average for the Λ production rate [9], this is equivalent to an Ω^- rate of $(1.2 \pm 0.5) \times 10^{-3}$ per event. The signal reported by TPC [7] at centre-of-mass energies of 29 GeV is equivalent to $(2.7^{+1.8}_{-1.1} \pm 0.8) \times 10^{-2}$ per event, or more than an order of magnitude larger.

Finally, in the invariant $\Lambda\gamma_C$ mass distribution (Figure 6), where γ_C is a converted photon reconstructed from e^+e^- pairs forming secondary vertices, 53 ± 10 events are observed at the

Σ^0 mass. The product of conversion probability times reconstruction efficiency is only a few percent, but the excellent resolution for the photon energy results in a detectable signal with a RMS width of only 2.7 ± 0.5 MeV/c^2. The acceptance corrected ratio of Σ^0 to Λ production is determined to be $0.33^{+0.11}_{-0.09}$.

In summary, the enhancement of baryon production in $\Upsilon(1S)$ decays is seen to hold also for the heavier Ξ^- and $\Xi^{*0}(1530)$ states. Evidence for decuplet production has been observed, at rates in the case of the $\Xi^{*0}(1530)$ well above previous limits from CLEO [8], and for the $\Sigma^{*\pm}$ well below the reported value from TPC [7].

3. The decay $D^0 \to \overline{K}^0\phi$

The decay $D^0 \to \overline{K}^0\phi$ was first observed by the ARGUS Collaboration in 1985 [10] with the unexpectedly large branching ratio of $BR(D^0 \to \overline{K}^0\phi) = (1.43 \pm 0.45)\%$. This showed that indeed the W-exchange diagram is very important, despite the fact that this process should be helicity and colour suppressed, and so can probably account for the observed lifetime differences between charged and neutral D-mesons. In view of the importance of this decay, we have repeated the analysis with a much larger data sample including the luminosity accumulated during 1985. The new ARGUS vertex chamber [11] was operational for about 50 pb^{-1} of this running, thus resulting in a considerable improvement of data quality, most notably, a 60% increase in the efficiency for reconstructing K^0_S's from secondary vertices.

Using standard criteria for event selection and particle identification [2], we obtain the invariant $K^0_S K^+ K^-$ mass spectrum shown in Figure 7, which exhibits a clean D^0 signal of 205 ± 38 events at a mass of (1864.3 ± 1.5) MeV/c^2, with a RMS width of (7.3 ± 1.5) MeV/c^2. No further cut is applied. The 2-body contributions to the 3-body decay $D^0 \to \overline{K}^0 K^+ K^-$ can be determined by investigating the K^+K^- subsystem. By requiring $|M(K^0_S K^+ K^-) - M(D^0)| < 16.2$MeV/$c^2$ we obtain the K^+K^- invariant mass spectrum shown in Figure 8 (points with error bars). Clearly visible is a prominent ϕ signal at the correct mass with the expected shape. Only the range up to a K^+K^- mass of 1.1 GeV/c^2 is shown, but this region contains most of the signal, namely 184 ± 25 events. The part of the K^+K^- mass spectrum which is not correlated with the $D^0 \to K^0_S\phi$ decay is determined from the sidebands above and below the D^0 (hatched histogram). There is a weak uncorrelated ϕ signal on a phase-space background, but a clear excess exists on the D^0.

A further demonstration that indeed the decay $D^0 \to K^0_S\phi$ has been observed is the distribution of the helicity angle θ, where θ is the angle between the K^+ and the K^0_S in the

rest frame of the ϕ meson. This distribution is shown in Figure 9 for the decay $D^0 \to K^0_S K^+ K^-$ where the K^+K^- invariant mass lies in the ϕ range. Acceptance is known from Monte Carlo studies to be constant in the whole angular range. The observed distribution exhibits the expected $\cos^2\theta$ behaviour, allowing for only a small s-wave contribution for K^+K^- masses below the ϕ. The dependence on $\cos^2\theta$ is also reflected in the Dalitz-plot (Figure 10) As a final consistency check, we have used D^0 mesons produced in the decay $D^{*+} \to D^0\pi^+$, where $D^0 \to K^0_S K^+ K^-$. We find 52 ± 9 events in the D^{*+} peak (Figure 11). The K^+K^- mass spectrum for these events again shows a strong ϕ peak above a much broader contribution which peaks near threshold and then falls off rapidly (Figure 12). The hatched histogram in the figure represents the background contribution, as determined from the D^{*+} sidebands. It is evident that one way to describe the non-ϕ contribution to the decay $D^0 \to K^0_S K^+ K^-$ is with a broad K^+K^- threshold effect, for example by the decay $D^0 \to K^0_S\delta(980)$.

A fit to the data with two Breit-Wigner resonances for the ϕ and the δ, using fixed masses and widths [12] folded with the known detector resolution function, describes the observed mass distribution quite well (solid curve in Figure 8). No acceptance corrections have to be applied since the acceptance is constant over the whole K^+K^- mass range. On the basis of this fit and the analysis of the $\cos\theta$ distibution, we find that $(46 \pm 7)\%$ of all $D^0 \to K^0_S K^+ K^-$ decays proceed via $D^0 \to K^0_S\phi$ and the remaining fraction is compatible with $D^0 \to K^0_S\delta(980)$. If one restricts this analysis to the ϕ region, with $1.01 < M(K^+K^-) < 1.03$ GeV/c^2, one finds that $(79 \pm 5)\%$ of all events in this range are due to the $D^0 \to K^0_S\phi$ decay. The branching ratio for the decay $D^0 \to K^0_S\phi$ can be determined by a comparison with the simultaneously measured, and well established, decay $D^0 \to K^0_S\pi^+\pi^-$ which has a branching ratio of $Br(D^0 \to \overline{K}^0\pi^+\pi^-) = (7.6 \pm 0.7 \pm 0.8)\%$ [13]. We then find:

$$\frac{Br(D^0 \to K^0_S\phi)}{Br(D^0 \to K^0_S\pi^+\pi^-)} = 0.155 \pm 0.033$$

$$Br(D^0 \to \overline{K}^0\phi) = (1.18 \pm 0.25 \pm 0.17)\%$$

For the remaining fraction of the $D^0 \to K^0_S K^+ K^-$ decay which might be completely due to the decay $D^0 \to K^0_S\delta(980)$, we obtain

$$Br(D^0 \to \overline{K}^0(K^+K^-)_{non-\phi}) = (0.64 \pm 0.15 \pm 0.09)\%$$

The second error in these branching ratios reflects the uncertainty in the $D^0 \to \overline{K}^0\pi^+\pi^-$ branching ratio.

In summary, based on a factor of three increase in our statistics, we have confirmed the existence of the decay $D^0 \to \overline{K}^0\phi$ and find a branching ratio consistent with our previous measurement. The surprisingly large value for this branching ratio implies that soft gluons, needed to overcome colour and helicity suppression, are important in D^0 decays.

4. Decay of B mesons

The reconstruction of B mesons is of basic importance in understanding the features of heavy quark systems. First, it allows a determination of the masses of charged and neutral B mesons, and branching ratios for various decay channels. In addition, it is essential for obtaining tagged B mesons to study Kobayashi-Maskawa matrix elements, B^0-$\overline{B^0}$ mixing, and CP-violation, which are of fundamental interest.

Exclusive B decays through channels leading to a D^{*+} meson in the final state have been reconstructed. Specifically, the channels

$$B^0 \to D^{*+}\pi^-$$
$$B^0 \to D^{*+}\pi^-\pi^0$$
$$B^0 \to D^{*+}\pi^-\pi^-\pi^+$$
$$B^- \to D^{*+}\pi^-\pi^-$$
$$B^- \to D^{*+}\pi^-\pi^-\pi^0$$

have been used. The D^{*+} is detected via its decay into $D^0\pi^+$, where the D^0 is reconstucted via the channels:

$$D^0 \to K^-\pi^+$$
$$D^0 \to K^0_S\pi^+\pi^-$$
$$D^0 \to K^-\pi^+\pi^0$$
$$D^0 \to K^-\pi^+\pi^+\pi^-.$$

Thus in total, 20 decay chains have been investigated. To improve the resolution on the mass of the B mesons, we performed mass constraint fits to the intermediate states, that is D^{*+}, D^0, K^0_S and π^0.

In the search for B candidates, two principal cuts were used:

1 We required the probability calculated for the sum of all χ^2 contributions from particle identification and kinematical fitting to exceed 1%.

2 We applied a beam-energy constraint fit to those B-candidates where $|E(B) - E(Beam)| < 3\sigma$. Such a fit translates the rather good momentum resolution for the B mesons into a good mass resolution without biasing the background distribution.

The mass spectrum for events satisfying these requirements is shown in Figure 13. We observe a signal of 71 ± 11 events at a mass of (5277.1 ± 0.8) MeV/c^2 with a width of $\sigma = 4.5$ MeV/c^2. The mass values given in the text are obtained by using a beam energy scale which sets the mass of the Υ(4S) to 10577 MeV/c^2 [14]. In the figures, a DORIS beam energy scale is used which differs by 2 MeV.

The shape of the combinatorial background was determined from event mixing (Figure 14), wrong charge combinations and from the mass distribution obtained in the continuum below the Υ(4S). It can be described by the form:

$$\frac{dN}{dM} \sim M \times \sqrt{1 - \frac{M^2}{E^2_{beam}}}$$

which can be derived assuming the background is uniformly distributed in phase space. The sample is shown separately for neutral and charged B mesons in Figures 15 and 16 respectively. From separate fits to these distributions, we find 40 ± 8 B^0's with a mass of $(5278.2 \pm 1.0 \pm 3.0)$ MeV/c^2 and 32 ± 7 B^-'s with a mass of $(5275.8 \pm 1.3 \pm 3.0)$ MeV/c^2 . If we discard decay chains with large combinatorical background we find a very clean B sample of about 30 events (Figure 17), which can be used for tagging purposes.

In order to determine branching ratios, we assume that 50% of the Υ(4S) decay into B^+B^- pairs and 50% into $B^0\overline{B^0}$ pairs. The branching ratios of the D^0 decay channels are taken from ref. 13 and 15. The number of events observed in the 5 decay channels and the corresponding branching ratios are given in the Table 2:

	number of events	branching ratio
$\overline{B^0} \to D^{*+}\pi^-$	5 ± 2.5	$(0.2 \pm 0.1 \pm 0.1)\%$
$\overline{B^0} \to D^{*+}\pi^-\pi^0$	8 ± 4	$(1.0 \pm 0.5 \pm 0.6)\%$
$\overline{B^0} \to D^{*+}\pi^-\pi^-\pi+$	27 ± 7	$(2.2 \pm 0.6 \pm 1.0)\%$
$B^- \to D^{*+}\pi^-\pi^-$	7 ± 3	$(0.4 \pm 0.2 \pm 0.2)\%$
$B^- \to D^{*+}\pi^-\pi^-\pi^0$	24 ± 7	$(3.8 \pm 1.1 \pm 2.2)\%$

Table 2. Observed number and branching ratios for B-meson decays.

A comparison with results so far published by the CLEO collaboration [16] on the decays $\overline{B^0} \to D^{*+}\pi^-$ and $B^- \to D^{*+}\pi^-\pi^-$ shows strong disagreement. The decay rates for these channels are about an order of magnitude smaller than the corresponding CLEO results ; only a factor of 2 can be explained as a consequence of recent changes in D^0 branching ratios. Specifically, if one considers only those decay chains analysed by both groups, one finds 11 CLEO events vs. 1 ARGUS event despite the fact that, for the two groups, the integrated luminosities are comparable (40 pb^{-1} and 59 pb^{-1} respectively) as are the acceptances.

The decay B → Charmonium + X can only proceed via the spectator diagram shown in Figure 18, and is therefore of interest as a test of colour suppression in B decays. Initial studies from ARGUS [17] gave a branching ratio $Br(B \to J/\Psi X) = (1.37^{+0.6}_{-0.5})\%$, based on an integrated luminosity of 12 pb^{-1} on the $\Upsilon(4S)$. With 5 times as much data now available, a more detailed picture of the decay B → Charmonium + X can be obtained. Figure 19 shows the invariant mass spectrum for e^+e^- or $\mu^+\mu^-$ pairs for events in the $\Upsilon(4S)$ region. The observed J/Ψ signal of 52±9 events at $M(e^+e^-,\mu^+\mu^-) = (3092 \pm 9)$ MeV/c^2 yields a (preliminary) new branching ratio $Br(B \to J/\Psi X) = (1.15 \pm 0.22 \pm 0.20)\%$, in good agreement with the previous result.

Visible at the mass of the Ψ', is an accumulation of about 5 events from the decay $B \to \Psi' X$. In order to check this hypothesis, we have studied the invariant $J/\Psi\pi^+\pi^-$ mass spectrum (Figure 20). From the known branching ratio for $\Psi' \to J/\Psi\pi^+\pi^-$, we expect to find about 5 events, which indeed are observed. On the basis of these numbers, we determine a branching ratio $Br(B \to \Psi' X) = (0.57 \pm 0.26)\%$. Thus, roughly 25% of the decay $B \to J/\Psi X$ is due to $B \to \Psi' X$, with the Ψ' decaying to the J/Ψ.

The fact that not all J/Ψ mesons are produced directly might lead to a softer momentum distribution for J/Ψ mesons from inclusive B meson decays. If the light quark in the B meson is treated as a spectator, one would naively expect from kinematics that the momentum spectrum is rather hard, unless dominated by high multiplicity channels. The observed spectrum is in fact surprisingly soft (Figure 21) and not quite consistent with a naive spectator picture.

B mesons can be reconstructed rather efficiently using the inclusive $B \to J/\Psi X$ events, since the recoil system X must contain a kaon and only a few π's, phase space being relatively limited. So far, we have reconstructed 9 B meson candidates in 4 different channels (Figure 22). The mass of B^0 mesons has been measured using the decay modes $B^0 \to \psi K^-\pi^+$ and

$B^0 \to \psi K^0_S\pi^+$. The result $M(B^0) = (5277 \pm 3 \pm 3)$ Mev/c^2 is entirely consistent with the value given above.

These first results fom ARGUS on reconstructed B mesons opens up the unique possibility of studying B mesons by using the tagging technique. Three new decay modes involving D^{*+} mesons have been observed for the first time as well as the decay $B \to \Psi' X$. It is remarkable that CLEO's value for the B-meson mass agrees reasonably well with ours in view of the fact that there is an order of magnitude discrepancy in the branching ratios for the channels upon which their mass was based.

5. The decay $\tau \to \omega\pi\nu$

One interesting τ decay, until now unobserved, is the decay $\tau \to \omega\pi\nu$. This channel is of special importance because it can proceed via a second-class axial-vector current if the $\omega\pi$ system forms a B(1235) meson, with $J^P = 1^+$ and $I^G = 1^+$. The observation of such a decay, $\tau \to B(1235)\nu$, would be the first manifestation of a second-class current.

Tau pairs were selected by requiring a 1-3 prong topology, with one π^0 on the 3-prong side and no π^0 on the 1-prong side or one π^0 on the 1-prong side which combines with the charged π to form a ρ meson. The resulting $\pi^+\pi^+\pi^-\pi^0$ mass distribution (Figure 23) contains 485 events, with a small background contribution of only 30 events below the τ mass. A plot of the invariant $\pi^+\pi^-\pi^0$ mass for these events shows an ω signal of 121±19 events at a mass of (783 ± 3.3) MeV/c^2 with an RMS width of (21 ± 3) MeV/c^2 (Figure 24). This is the first observation of the decay $\tau^+ \to \omega\pi^+\overline{\nu}$. We find that the $\tau^+ \to \omega\pi^+\overline{\nu}$ decay represents $(28.5 \pm 5.5)\%$ of the decay $\tau^+ \to \pi^+\pi^+\pi^-\pi^0\overline{\nu}$ yielding a (preliminary) branching ratio of $Br(\tau \to \omega\pi\nu) = (1.7 \pm 0.4)\%$ by taking a world average for the branching ratio for $\tau^+ \to \pi^+\pi^+\pi^-\pi^0\overline{\nu}$ of $(5.3 \pm 0.5)\%$.

The spin-parity of the $\omega\pi$ system can be determined from the distribution of the angle Ψ, the angle between the normal of the ω decay plane and the direction of the bachelor π in the rest system of the ω. (Figure 25). This distribution is obtained by fitting the number of ω 's in each bin of the angular distribution. It clearly favours a $J^P = 1^-$ assignment. This implies that second-class currents do not dominate the decay $\tau \to \omega\pi\nu$, and we find an upper limit of 50% at the 90% CL for $J^P = 1^+$ contributions to this channel.

The invariant $\omega\pi$ mass distribution in the decay $\tau \to \omega\pi\nu$ is obtained in a similar way to the angular distribution (Figure 26). No pronounced structure is visible, in particular in

the region of the B(1235) meson. We conclude that the $\tau \to \omega\pi\nu$ decay represents a sizeable fraction of the τ decays and that it proceeds mainly by a first-class vector current.

References

* Current members of the ARGUS collaboration are: H.Albrecht, U.Binder, P.Böckmann, R.Gläser, G.Harder, I.Lembke-Koppitz, A.Philipp, W.Schmidt-Parzefall, H.Schröder, H.D.Schulz, R.Wurth, A.Yagil (DESY), J.P.Donker, A.Drescher, D.Kamp, U.Matthiesen, H.Scheck, B.Spaan, J.Spengler, D.Wegener (Dortmund), J.C.Gabriel, K.R.Schubert, J.Stiewe, K.Strahl, R.Waldi, S.Weseler (Heidelberg), K.W.Edwards, W.R.Frisken, Ch.Fukunaga, D.J.Gilkinson, D.M.Gingrich, M.Goddard, H.Kapitza, P.C.H.Kim, R.Kutschke, D.B.MacFarlane, J.A.McKenna, K.W.McLean, A.W.Nilsson, R.S.Orr, P.Padley, P.M.Patel, J.D.Prentice, H.C.J.Seywerd, T.-S.Yoon, J.C.Yun (IPP Canada), R.Ammar, D.Coppage, R.Davis, S.Kanekal, N.Kwak (Kansas), G.Kernel, M.Pleško (Ljublijana), L.Jönsson (Lund), A.Babaev, M.Danilov, A.Golutvin, I.Gorelov, V.Lubimov, V.Matveev, V.Nagovitsin, V.Ryltsov, A.Semenov, V.Shevchenko, V.Soloshenko, V.Tchistilin, I.Tichomirov, Yu.Zaitsev (ITEP-Moscow), R.Childers, C.W.Darden, Y.Oku (South Carolina), and H.Gennow (Stockholm).

[1] I.Bigi and M.Fugugita, Phys.Lett. **91B** (1980) 121.

[2] M.Danilov et al., Nucl.Instr.Methods **217** (1983) 153;
R.Heller et al., Nucl.Instr.Methods **A235** (1985) 26;
A.Drescher et al., Nucl.Instr.Methods **205** (1983) 125, **216** (1983) 35 and **A237** (1985) 464;
A.Drescher et al., "Calibration and monitoring of the ARGUS shower counters", DESY preprint DESY 86-019 (1986);
A.Arefiev et al., DESY preprint DESY 83-025 (1983);
H.Albrecht et al. (ARGUS collaboration), Phys.Lett. **134B** (1984) 137 and **150B** (1985) 235.

[3] References to a specific charged state should be interpreted as implying the charge conjugate state also.

[4] C.W.Darden et al. (DASP II collaboration) Phys.Lett. **80B** (1979) 419.

[5] S.Behrends et al. (CLEO collaboration) Phys.Rev. **D31** (1985) 2161.

[6] M.Althoff et al. (TASSO collaboration) Z.Phys. **C26** (1984) 181.

[7] H.Aihara et al. (TPC collaboration), "Ξ^-, Σ^{*-} and Ω^- production in e^+e^- annihilation at 29 GeV", contributed paper to the European Physical Society Meeting on High Energy Physics, Bari (1985).

[8] M.S.Alam et al. (CLEO collaboration) Phys.Rev.Lett. **53** (1984) 24.

[9] D.H.Saxon, Proceedings of the European Physical Society Meeting on High Energy Physics, Bari (1985) 899.

[10] H.Albrecht et al. (ARGUS collaboration), Phys.Lett. **158B** (1985) 525.

[11] K.W.Edwards et al. (ARGUS collaboration), The ARGUS Vertex Drift Chamber, to appear in the Proceedings of the Wire Chamber Conference, Vienna (1986).

[12] Particle Data Group, Rev.Mod.Phys. **56** (1984) No.2, PartII.

[13] D.H.Coward et al. (MARK III collaboration) SLAC-PUB-3818 (1985).

[14] Particle Data Group, Phys.Lett. **170B** (1986) 1.

[15] R.M.Baltrusaitis et al. (MARK III collaboration), Phys.Rev.Lett. **56** (1986) 2140.

[16] R.Giles et al. (CLEO collaboration), Phys.Rev.D **30** (1984) 2279.

[17] H.Albrecht et al. (ARGUS collaboration), Phys.Lett. **162B** (1985) 395.

Figure captions

Figure 1 W-exchange diagram for the decay $D^0 \to \overline{K}^0\phi$.

Figure 2 $p\pi^-$ mass spectrum for events from e^+e^- interactions at center of mass energies around 10 GeV.

Figure 3a $\Lambda\pi^-$ mass spectrum. For the open histogram we required $\Lambda\pi^-$ momenta greater than 400 MeV/c, but with no vertex requirement for the π^-. For the hatched histogram we required that the $\pi^\pm$ fit to the primary event vertex, but applied no momentum cut.

Figure 3b $\Lambda\pi^+$ mass spectrum with requirement that the π^+ fit to the primary event vertex.

Figure 4 $\Sigma^-\pi^+$ mass spectrum.

Figure 5 ΛK^- mass spectrum.

Figure 6 $\Lambda\gamma_c$ mass spectrum.

Figure 7 $K^0_S K^+ K^-$ mass spectrum.

Figure 8 K^+K^- mass spectrum for events with $|M(K^0_S K^+ K^-) - M(D^0)| < 16.2$ MeV/c^2 (points with error bars). The hatched histogram gives the contribution which is not correlated with a D^0 meson.

Figure 9 Distribution of the helicity angle Θ in in the decay $D^0 \to K^0_S\phi, \phi \to K^+K^-$. The decay is defined by $|M(K^0_S K^+ K^-) - M(D^0)| < 16.2$ MeV/c^2 and $|M(K^+K^-) - M(\phi)| < 6.6$ MeV/c^2. The contribution to this angular distribution which is not correlated with a D^0 meson has already been subtracted.

Figure 10 Dalitz plot for events with $|M(K^0_S K^+ K^-) - M(D^0)| < 16.2$ MeV/c^2.

Figure 11 $D^0\pi^+$ mass spectrum with $D^0 \to K^0_S K^+ K^-$.

Figure 12 K^+K^- mass spectrum in the decay $D^{*+} \to D^0\pi^+$, $D^0 \to K^0_S K^+ K^-$ (open histogram) and from D^{*+} sidebands (hatched histogram).

Figure 13 Mass distribution of B meson candidates.

Figure 14 Mass distribution of background candidates obtained by event mixing.

Figure 15 Mass distribution of B^0 candidates.

Figure 16 Mass distribution of $B^{\pm}$ candidates.

Figure 17 Mass distribution of B candidates, selected decay chains.

Figure 18 Spectator diagram for the decay B → Charmonium + X.

Figure 19 e^+e^-, $\mu^+\mu^-$ mass spectrum for events taken at the $\Upsilon(4S)$.

Figure 20 $J/\Psi\pi^+\pi^-$ mass spectrum with $J/\Psi \to e^+e^-, \mu^+\mu^-$.

Figure 21 Momentum spectrum of J/Ψ mesons from $\Upsilon(4S)$.

Figure 22 Sum of mass spectra for the decays $B^0 \to J/\Psi + K^{*0}$ (5 events), $B^0 \to \Psi' + K^+\pi^-$ (1 event), $B^- \to J/\Psi + K^-$ (2 events) and $B^- \to \Psi' + K^-\pi^+\pi^-$ (2 events).

Figure 23 $\pi^+\pi^+\pi^-\pi^0$ mass spectrum in the decay $\tau^+ \to \pi^+\pi^+\pi^-\pi^0\bar{\nu}$.

Figure 24 $\pi^+\pi^-\pi^0$ mass spectrum in the decay $\tau^+ \to \pi^+\pi^+\pi^-\pi^0\bar{\nu}$.

Figure 25 Distribution of the angle Ψ in the decay $\tau^+ \to \omega\pi^+\bar{\nu}$.

Figure 26 $\omega\pi^+$ mass spectrum in the decay $\tau^+ \to \omega\pi^+\bar{\nu}$.

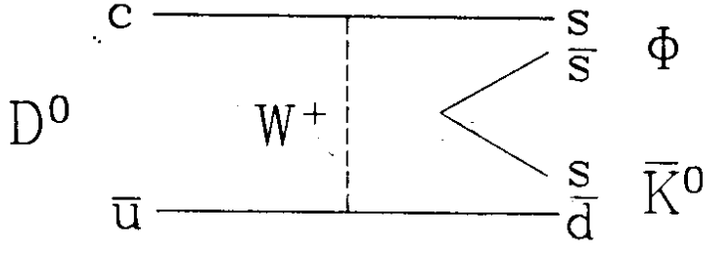

Figure 1

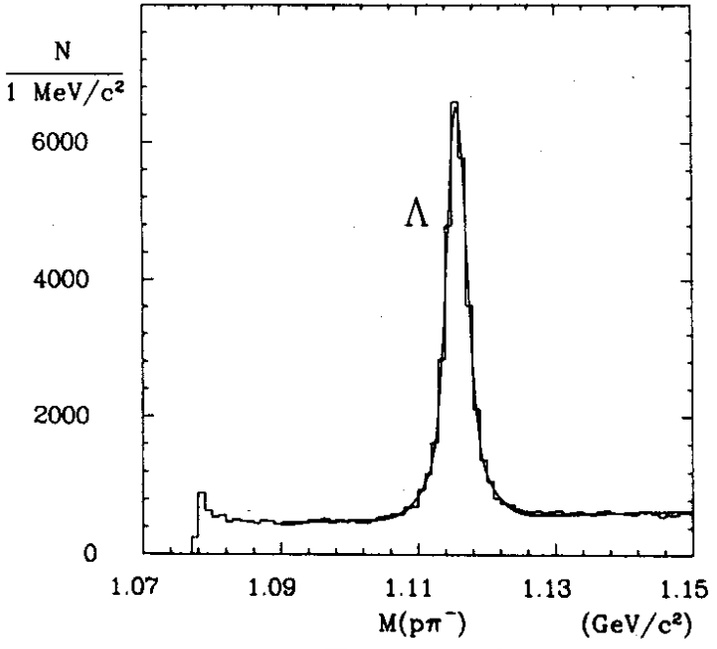

Figure 2

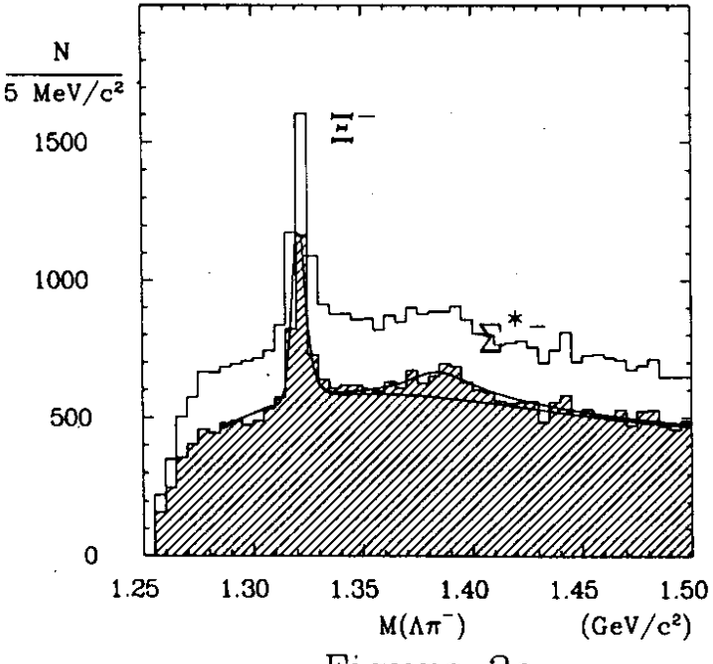

Figure 3a

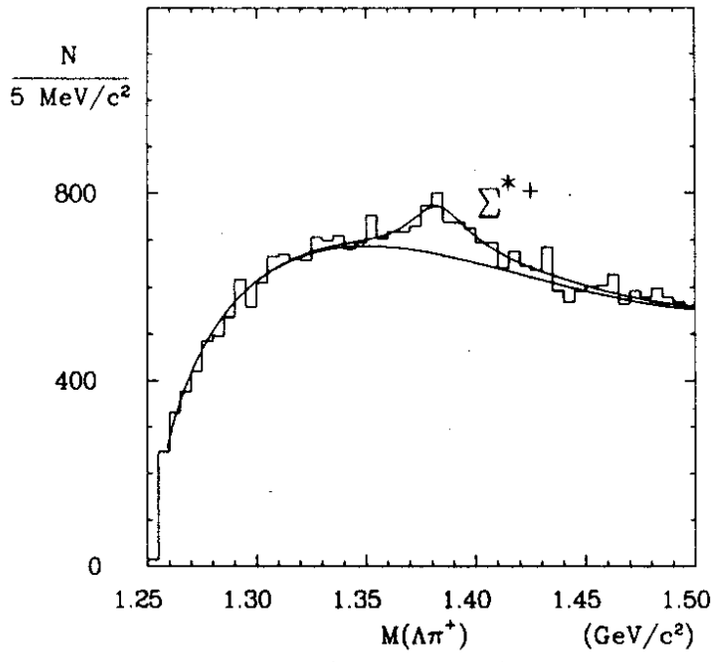

Figure 3b

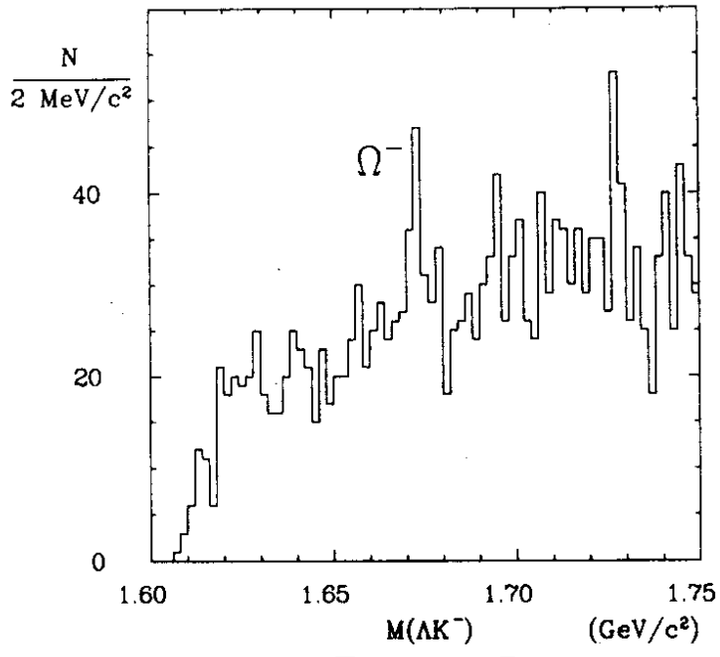

Figure 5

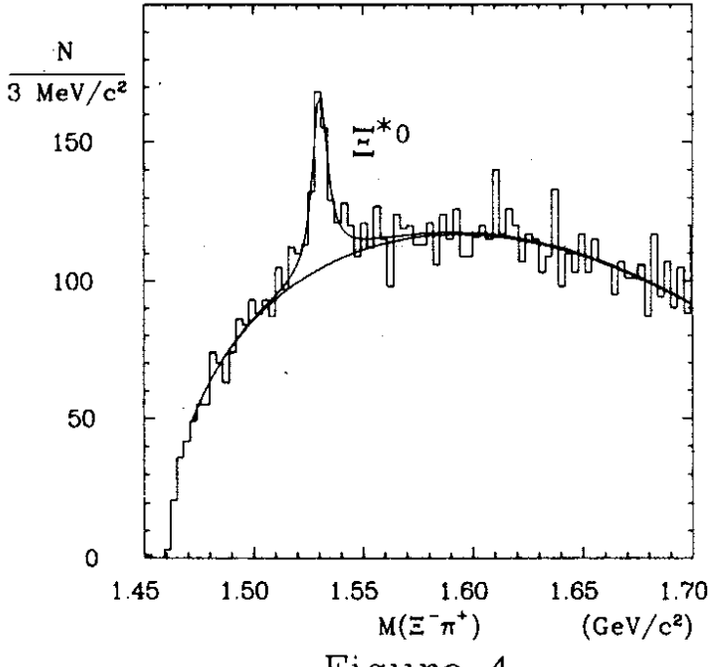

Figure 4

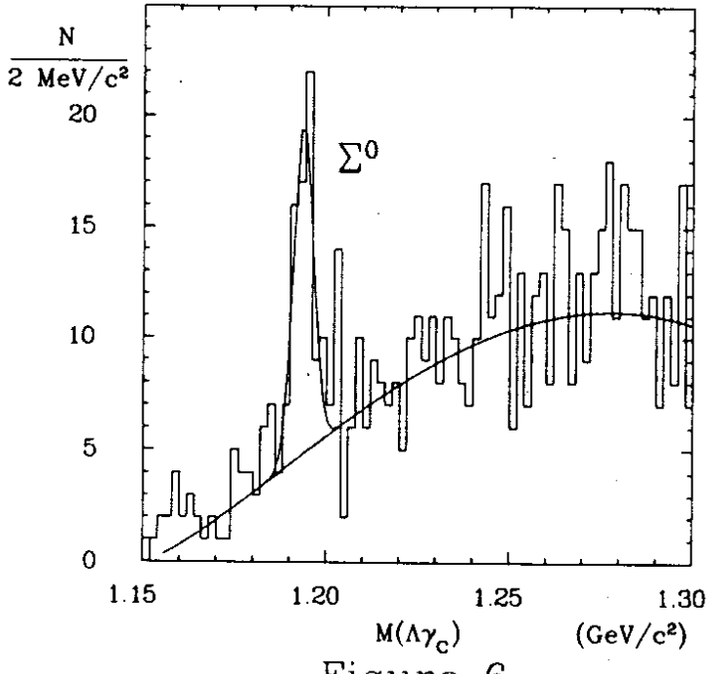

Figure 6

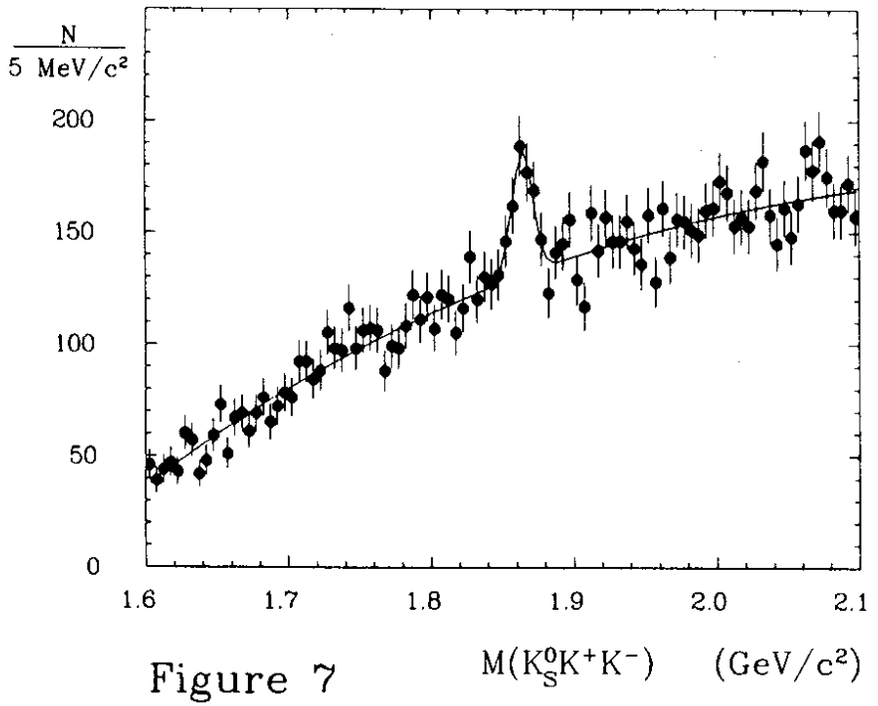

Figure 7

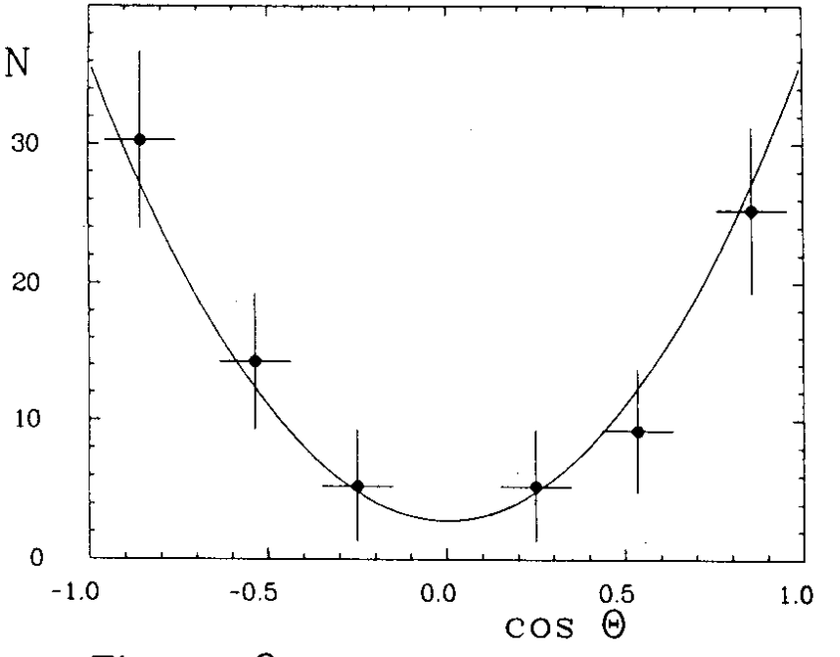

Figure 9

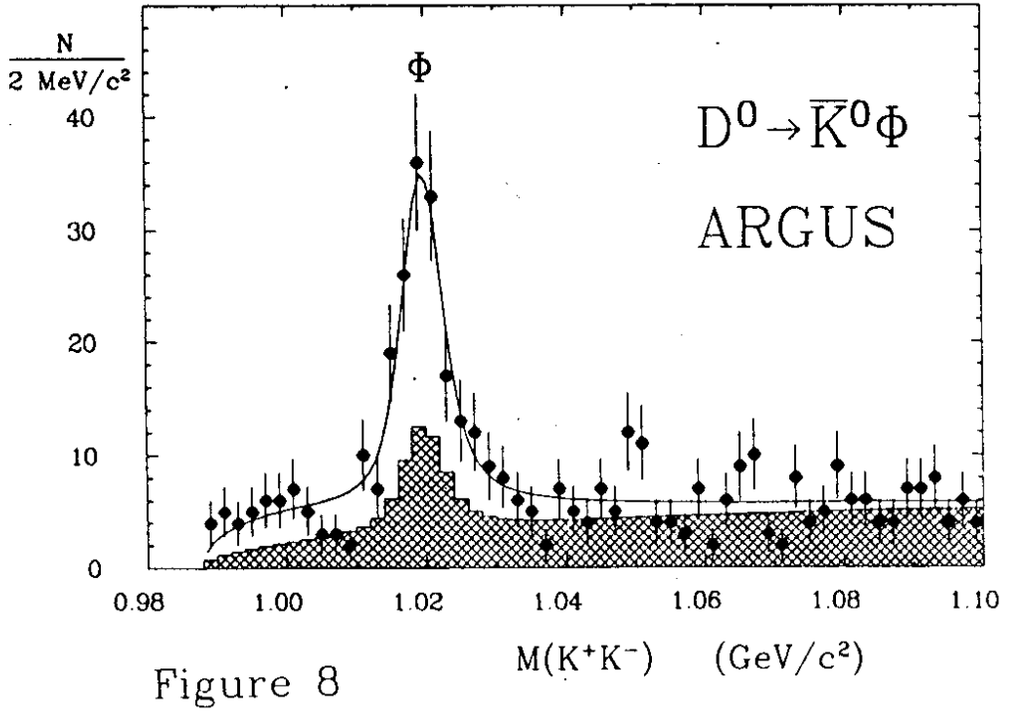

Figure 8

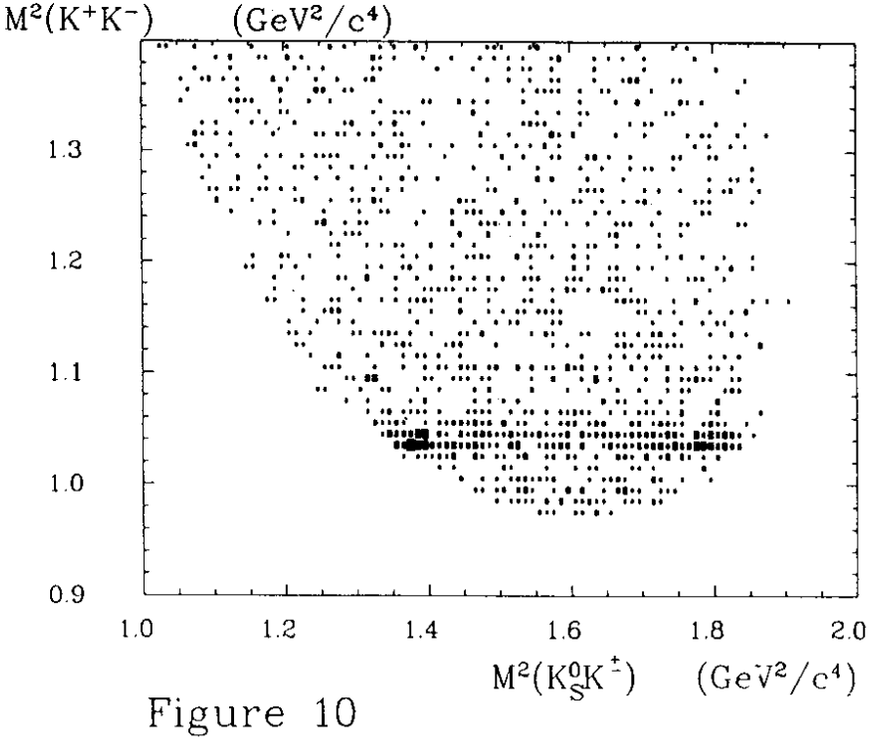

Figure 10

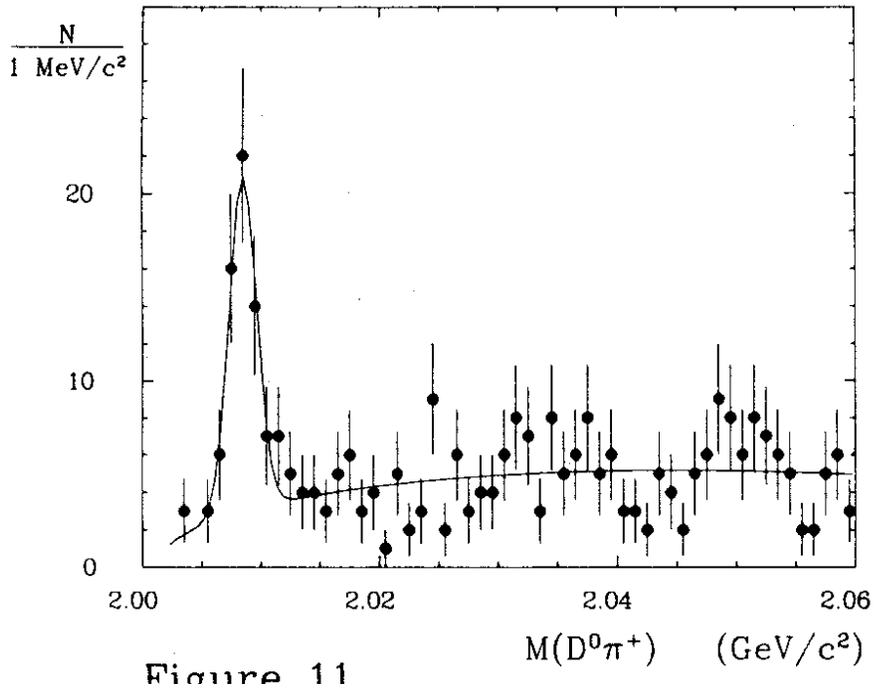

Figure 11

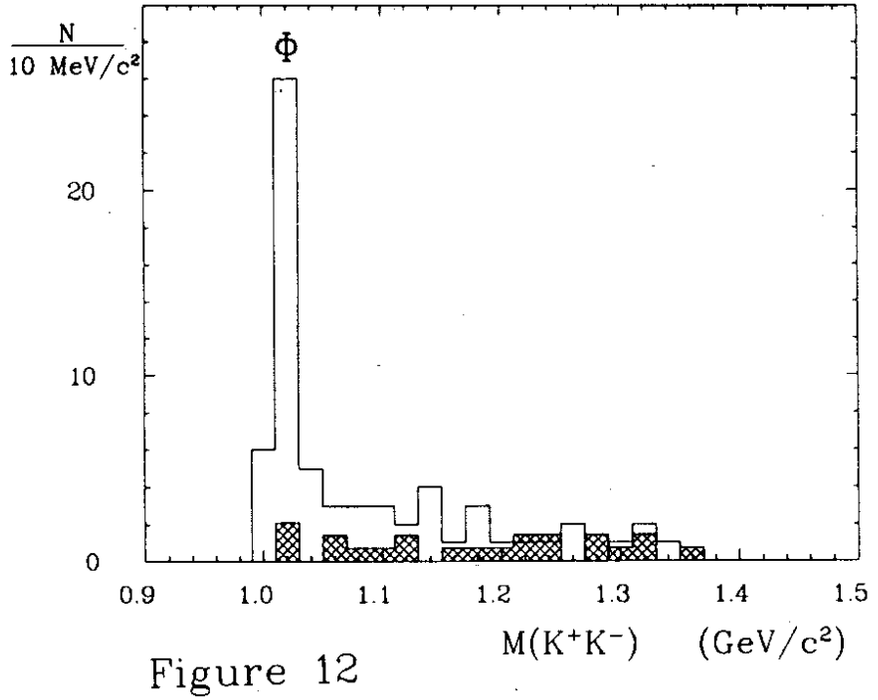

Figure 12

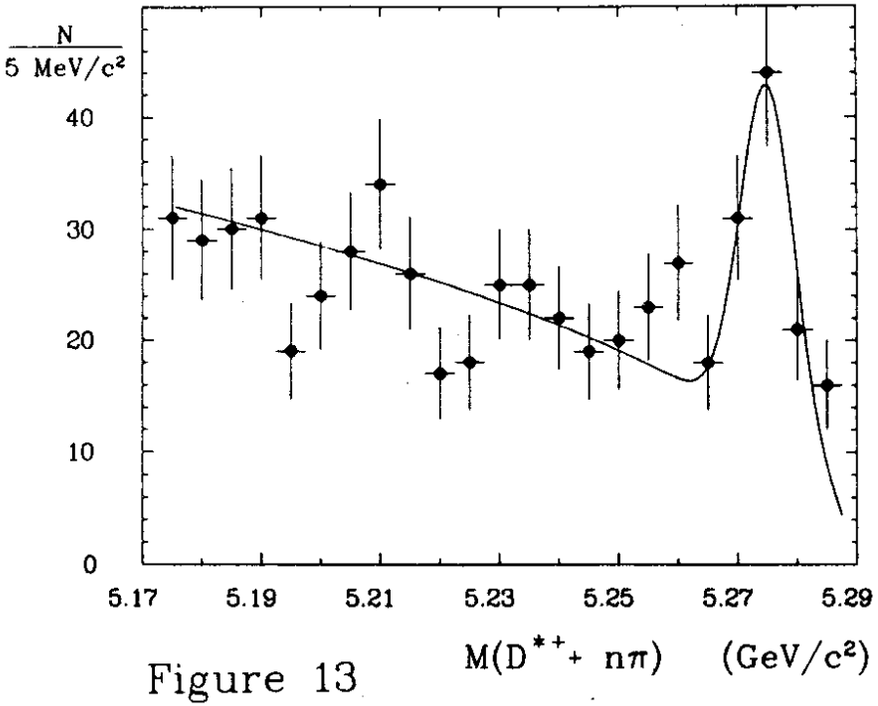

Figure 13

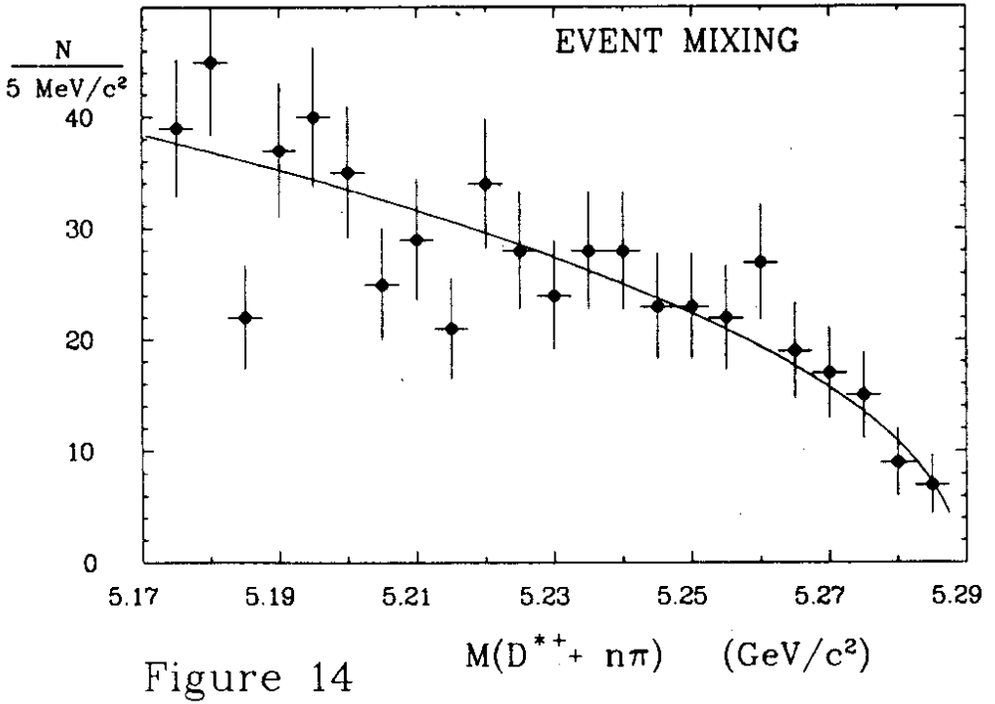

Figure 14

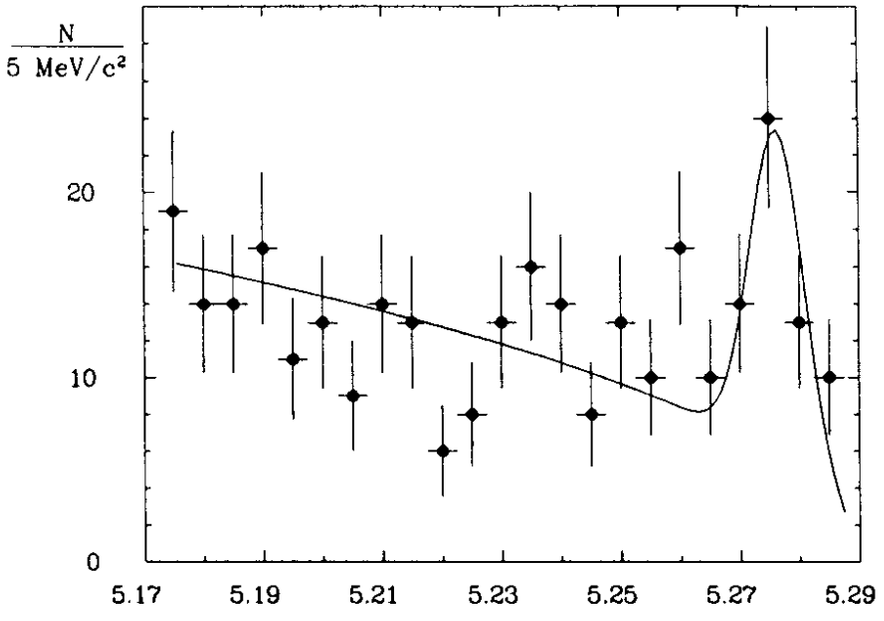

Figure 15

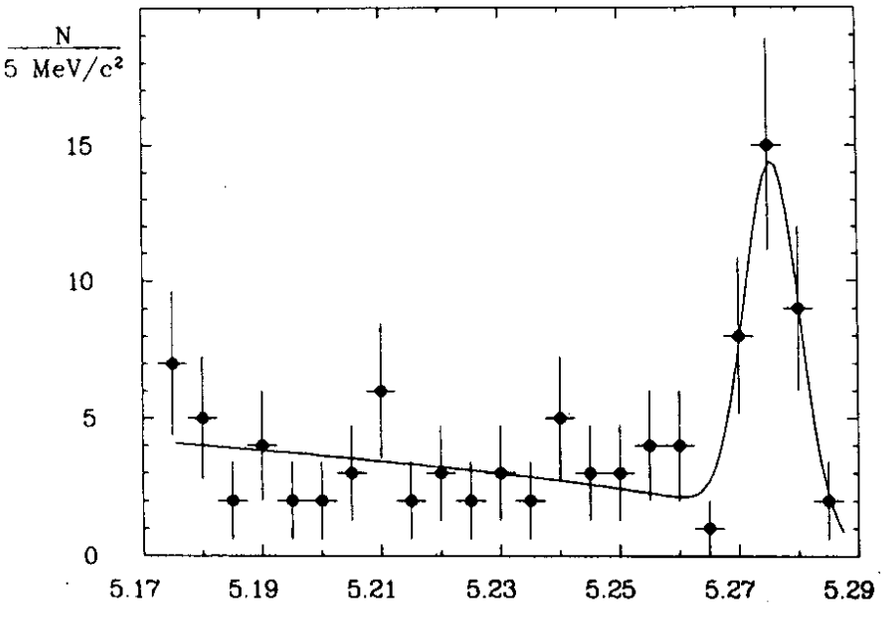

Figure 17

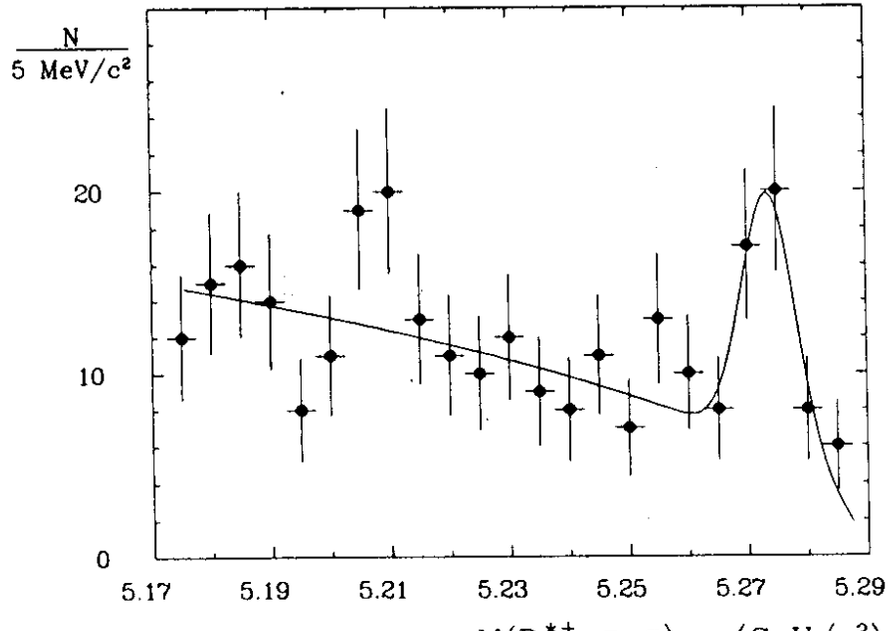

Figure 16

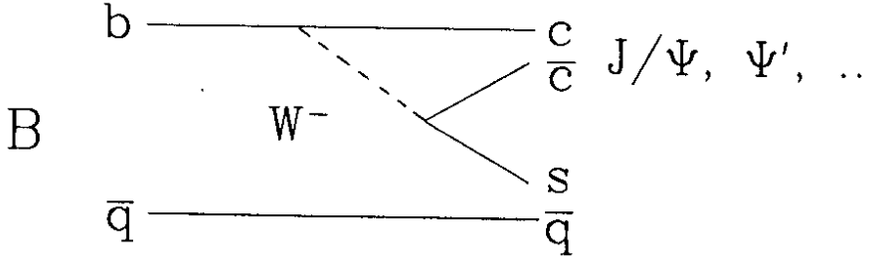

Figure 18

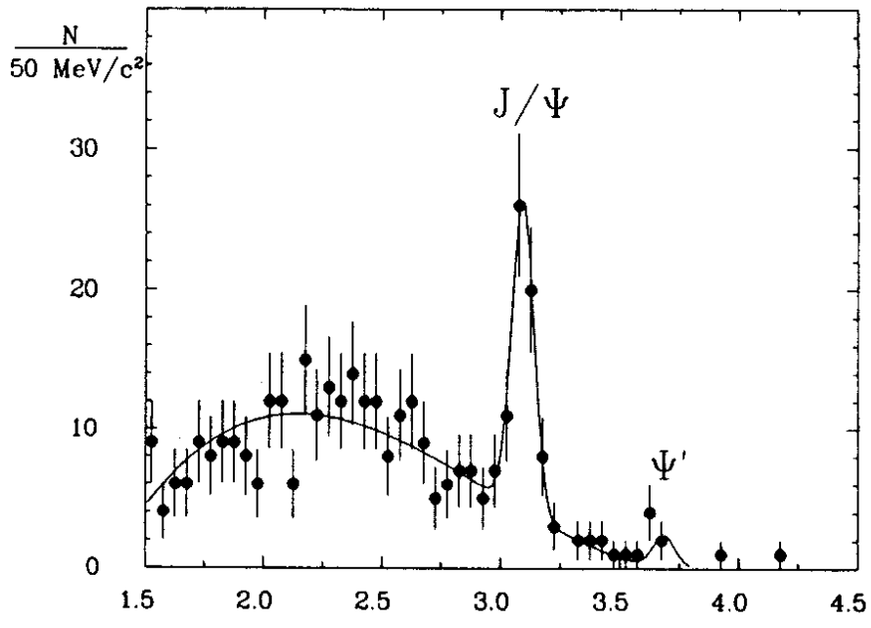

Figure 19

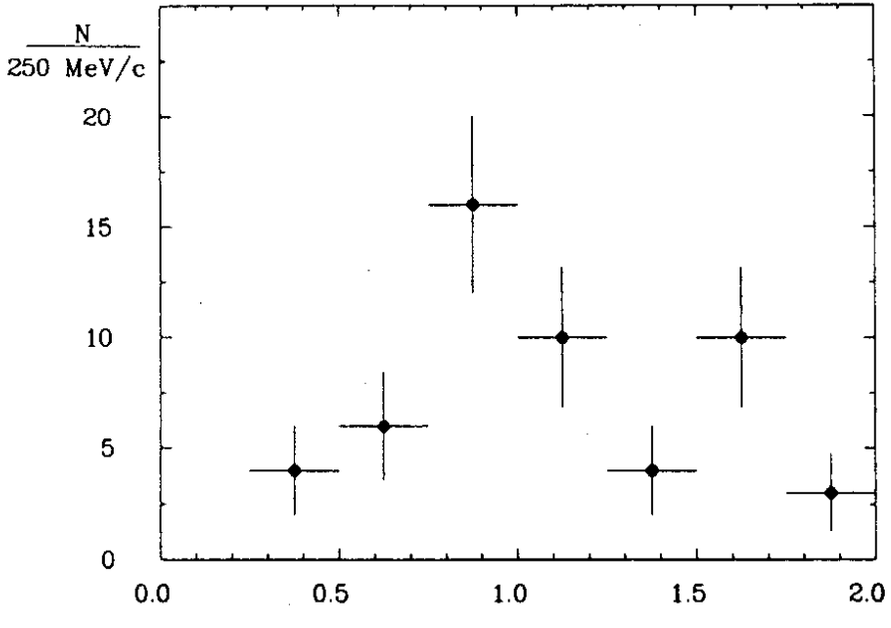

Figure 21

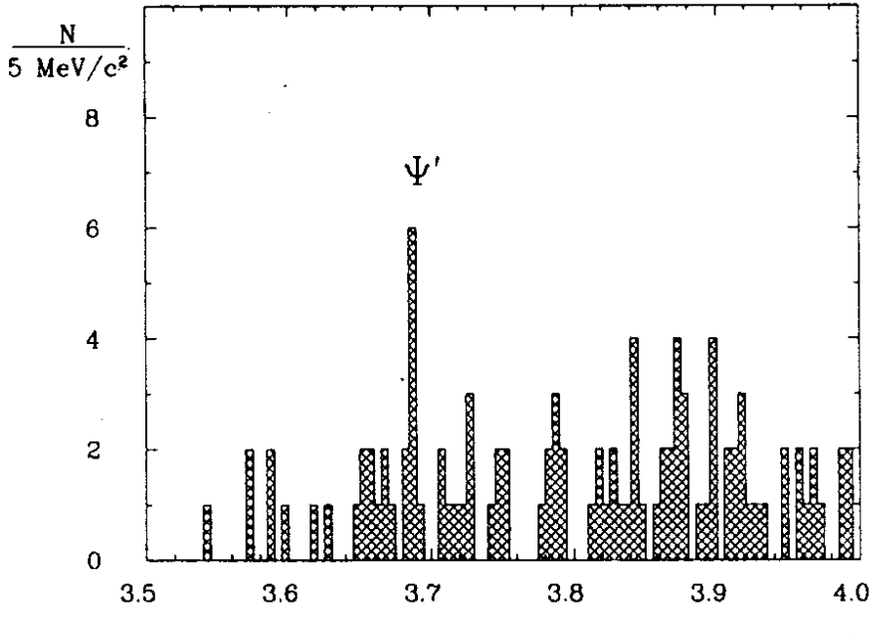

Figure 20

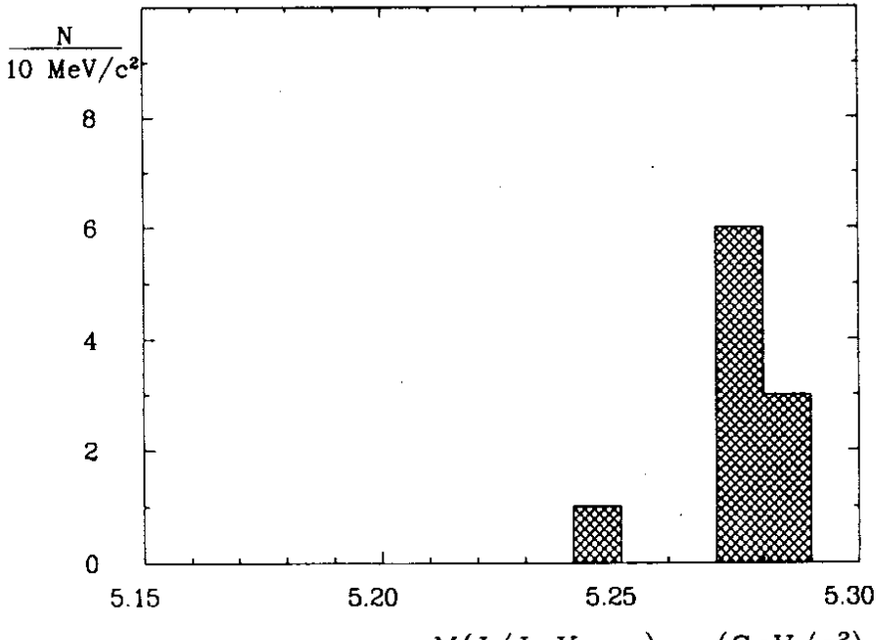

Figure 22

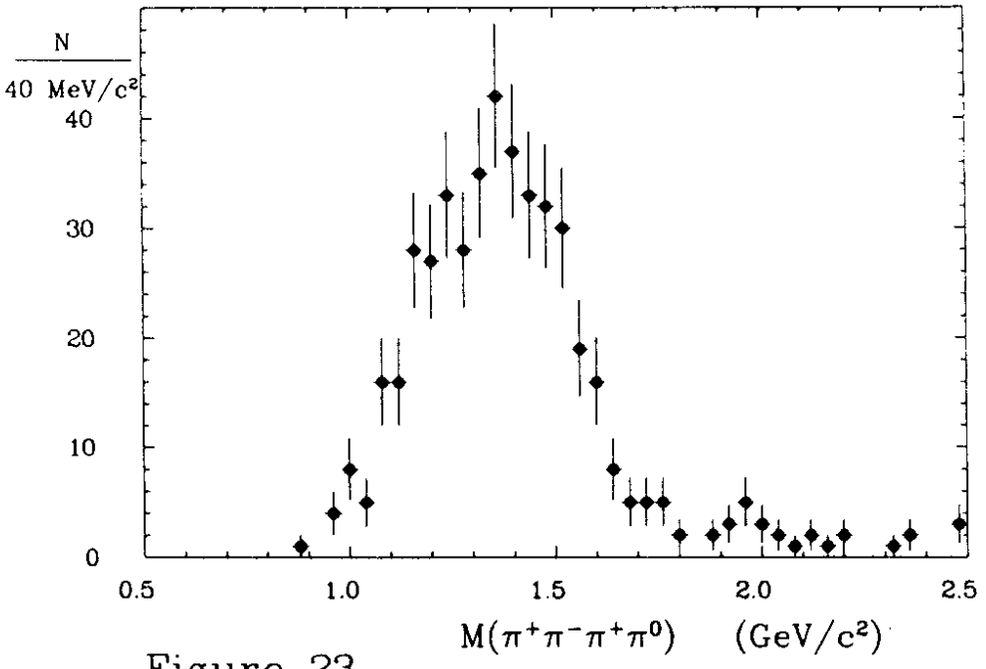

Figure 23

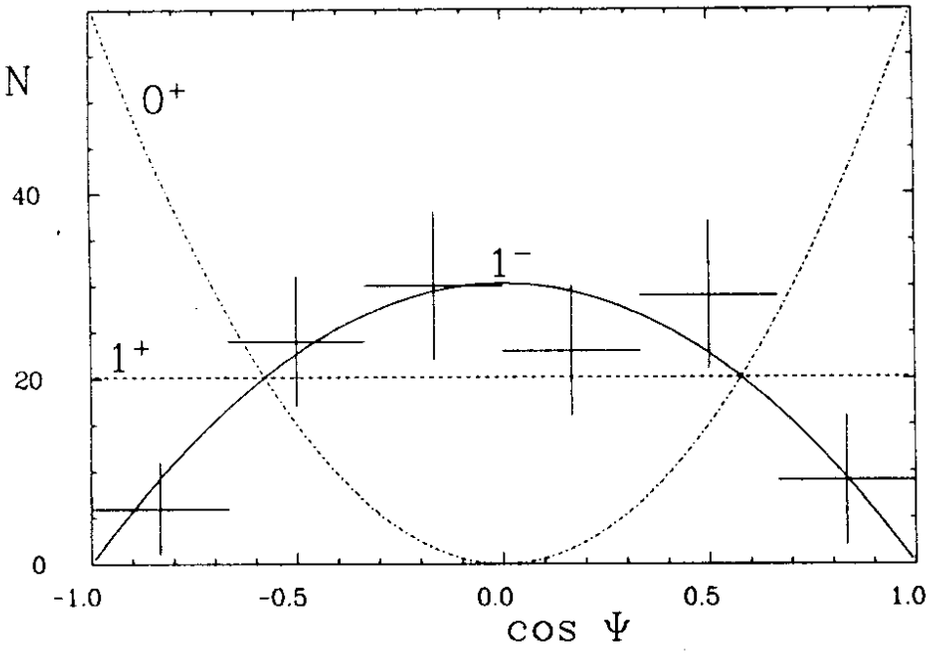

Figure 25

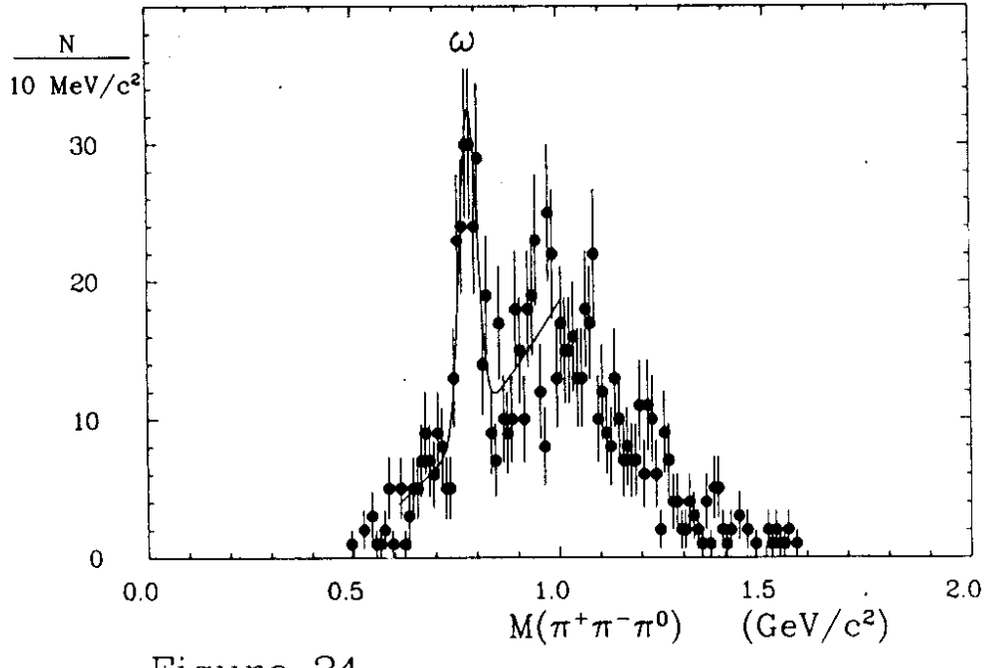

Figure 24

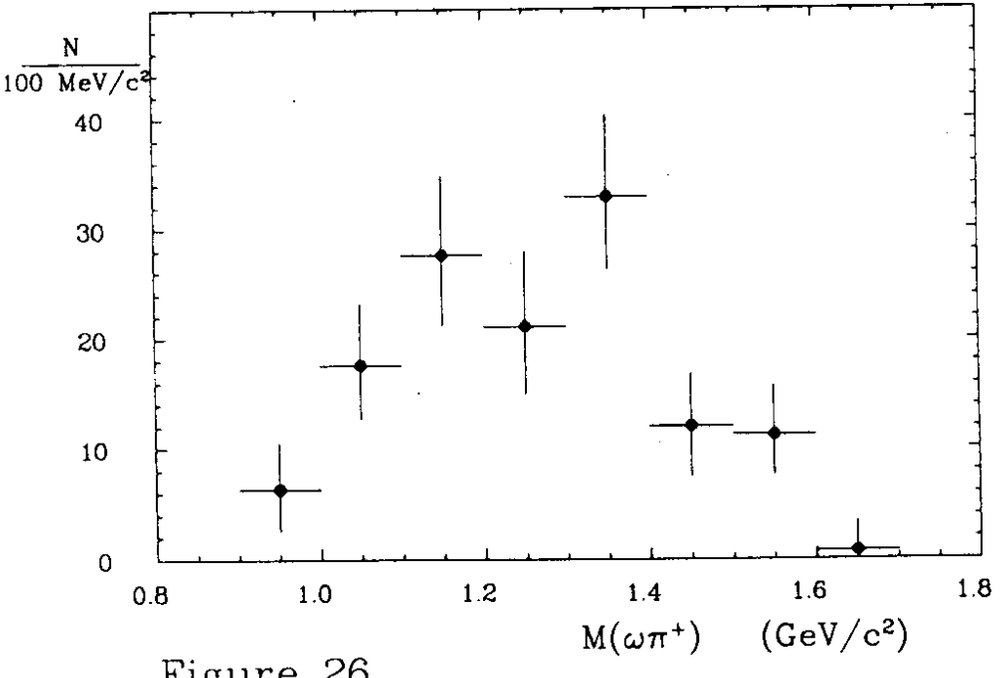

Figure 26